Supporting Information for

cPCN-Regulated SnO_2 Composites Enables Perovskite Solar Cell with Efficiency Beyond 23%

Zicheng Li[1, 2, 3], Yifeng Gao[1, 3], Zhihao Zhang[1, 2, 3], Qiu Xiong[1, 3], Longhui Deng[1, 3], Xiaochun Li[2], Qin Zhou[1, 3], Yuanxing Fang[2], Peng Gao[1, 3, *]

[1]CAS Key Laboratory of Design and Assembly of Functional Nanostructures, and Fujian Provincial Key Laboratory of Nanomaterials Fujian Institute of Research on the Structure of Matter, Chinese Academy of Sciences, Fuzhou, Fujian 350002, People's Republic of China

[2]College of Chemistry, Fuzhou University, Fuzhou 350116, People's Republic of China

[3]Laboratory for Advanced Functional Materials, Xiamen Institute of Rare Earth Materials, Haixi Institute, Chinese Academy of Sciences, Xiamen 361021, People's Republic of China

*Corresponding author. E-mail: peng.gao@fjirsm.ac.cn (Peng Gao)

Supplementary Figures and Tables

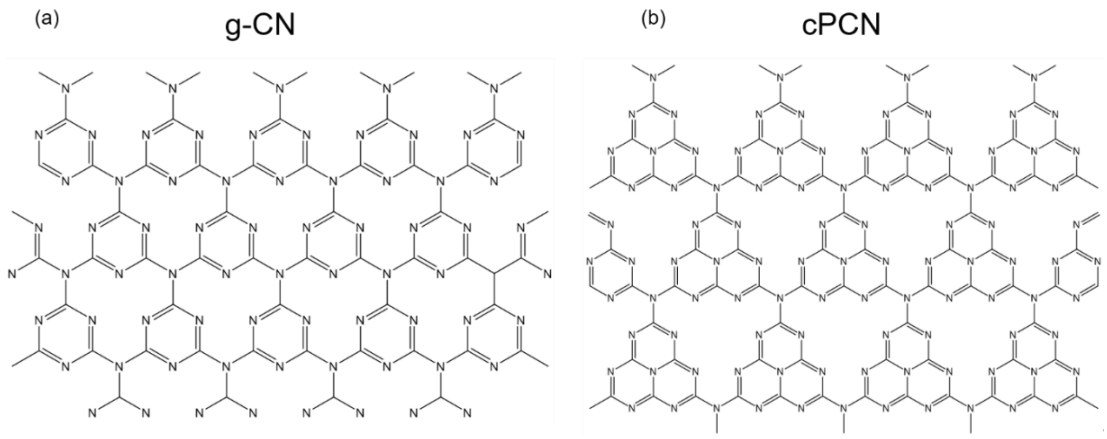

Fig. S1 Structure models of g-CN, cPCN

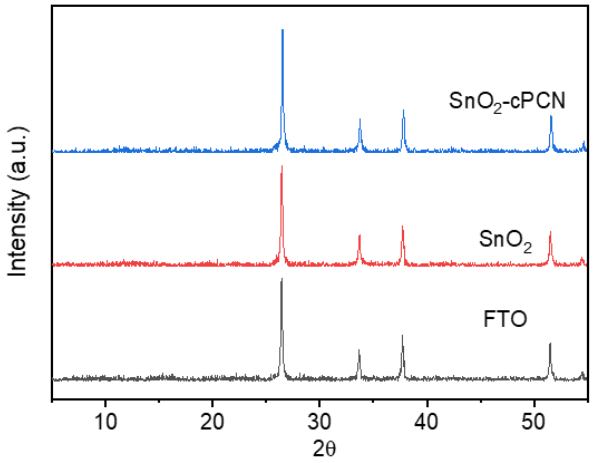

Fig. S2 XRD spectra of FTO, SnO_2 and SnO_2-cPCN

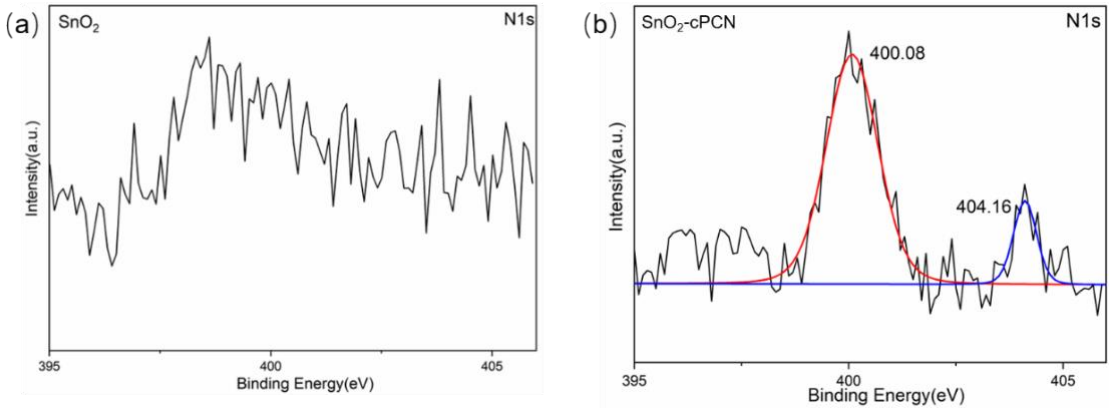

Fig. S3 XPS spectra of N 1s of **(a)** SnO_2 and **(b)** SnO_2-cPCN

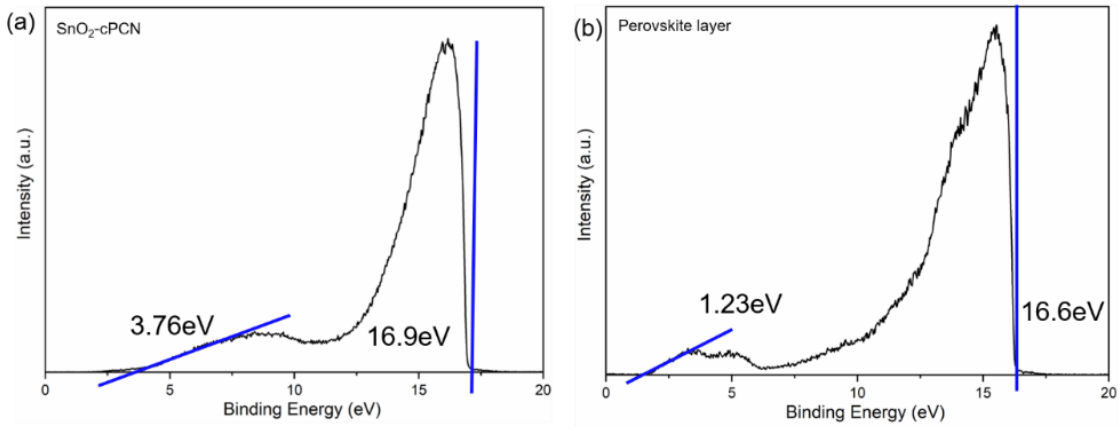

Fig. S4 UPS spectra for SnO_2-cPCN film and perovskite film deposited on glass

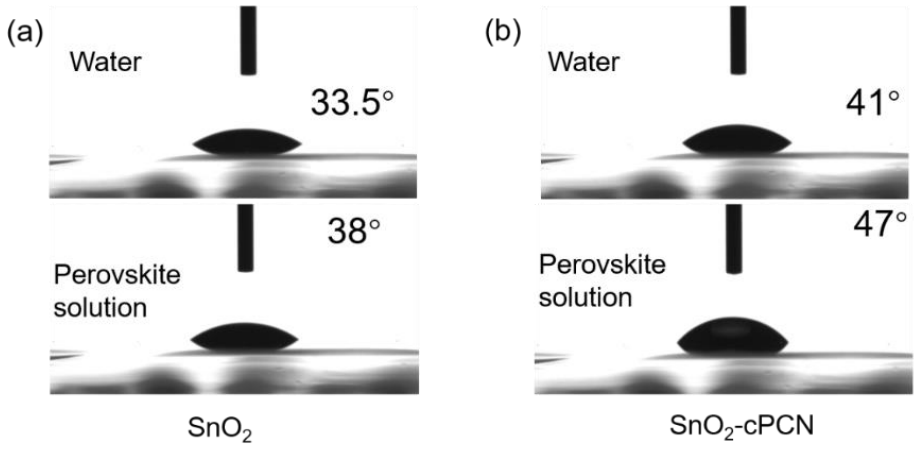

Fig. S5 Contact angle measurements of water and perovskite solution on SnO_2 and SnO_2-cPCN films

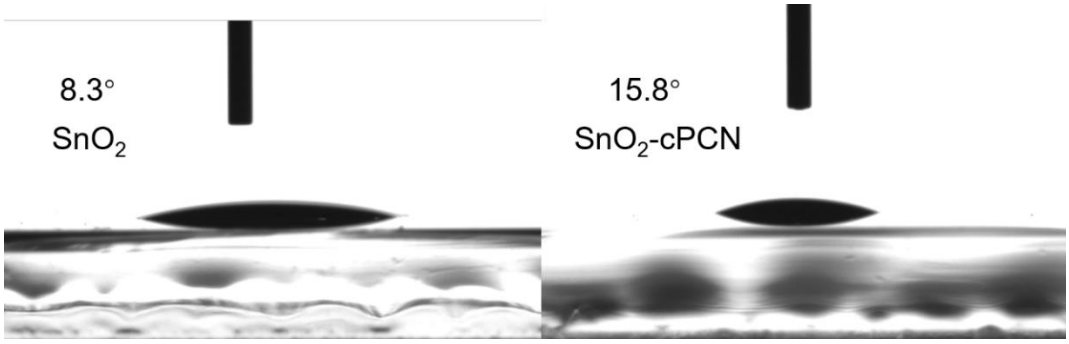

Fig. S6 Contact angle measurements of perovskite solution on SnO_2 and SnO_2-cPCN films after UV-ozone treatment

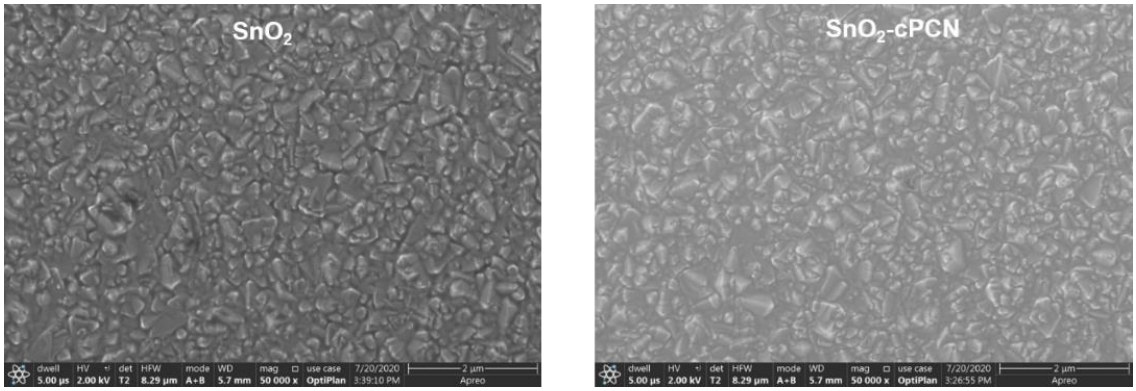

Fig. S7 SEM images of SnO_2 **(**Left**)** and SnO_2-cPCN film **(**Right**)**

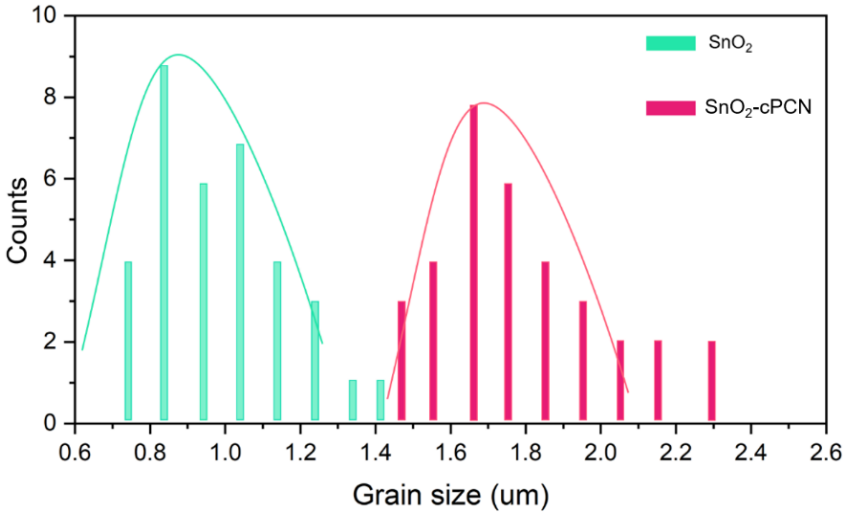

Fig. S8 Average grain size of the perovskite films on SnO_2 and SnO_2-cPCN derived from Fig 3a, b

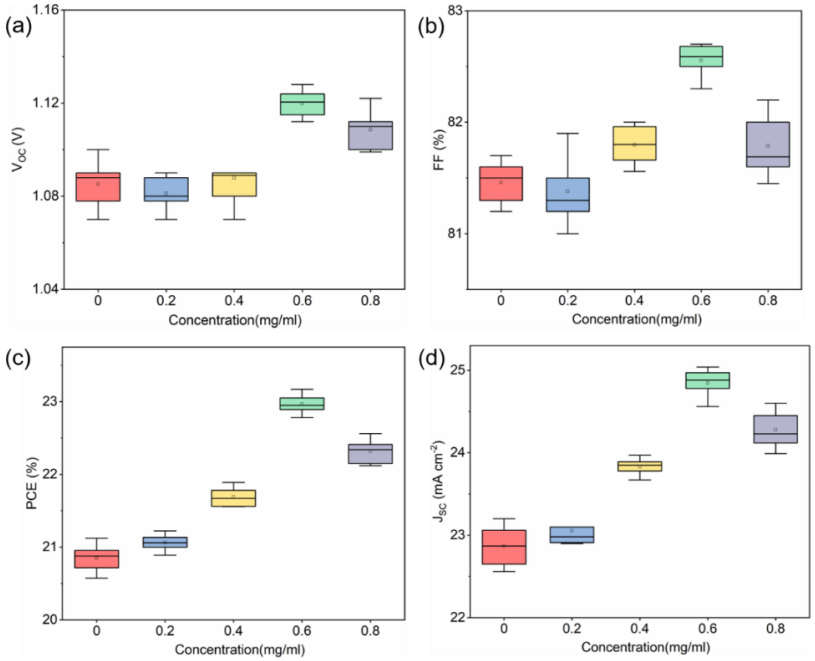

Fig. S9 (a-d) PCE, FF, V_{OC}, and J_{SC} extracted from their corresponding J-V curves as functions of the cPCN concentration in the SnO_2 solution for the preparation of SnO_2-cPCN ETL

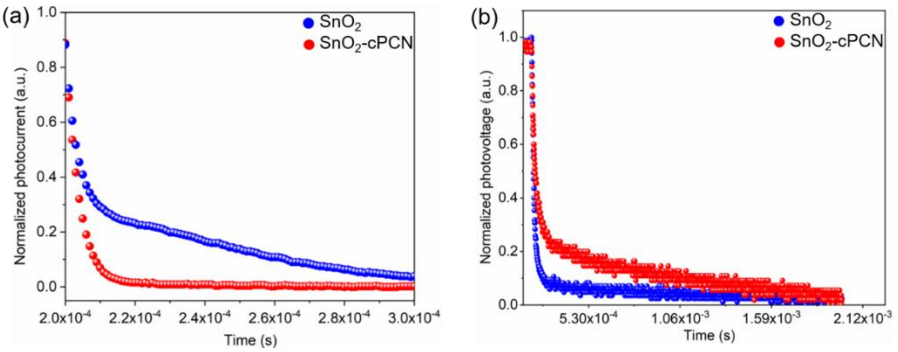

Fig. S10 (**a**) Normalized transient photocurrent decay and (**b**) normalized transient photovoltage decay of PSCs with SnO_2 and SnO_2-cPCN as ETL

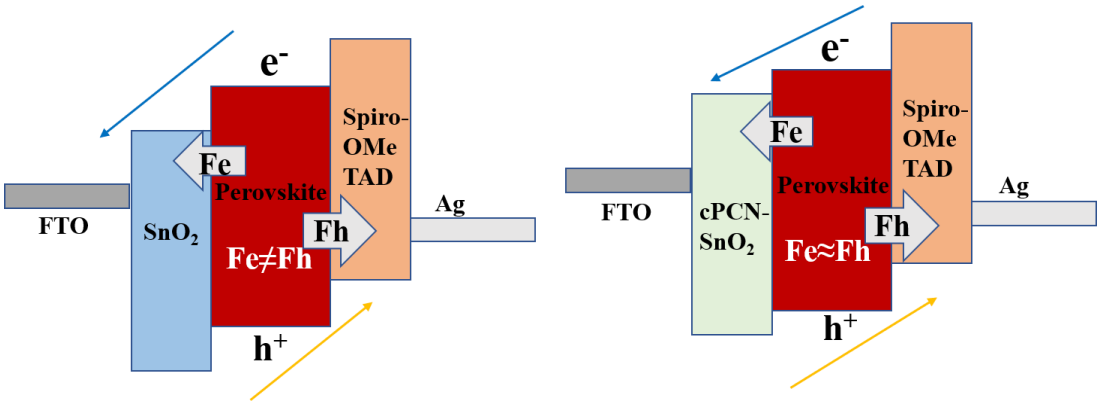

Fig. S11 Charge transport mechanism. (a) Planar-type PSCs with SnO_2 and (b) SnO_2-cPCN

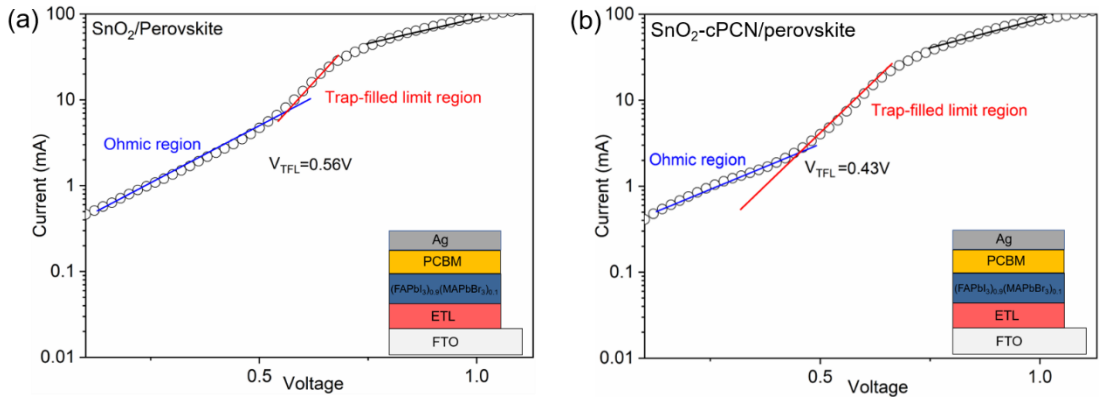

Fig. S12 Dark I–V curves of the electron-only devices with the V_{TFL} kink points. The inset shows the structure of the electron-only device

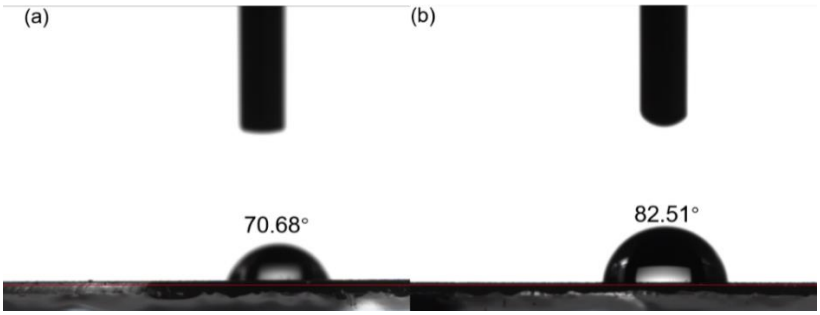

Fig. S13 Contact angle of perovskite film based on (**a**) SnO_2 and (**b**) SnO_2-cPCN

Table S1 Device performance of V_{OC}, J_{SC}, FF, and PCE of devices at different cPCN concentrations

Concentration(mg/ml)	Voc (V)	J_{SC} ($mAcm^{-2}$)	FF (%)	PCE (%)
0	1.11	23.2	82	21
0.2	1.11	23.5	81.5	21.5
0.4	1.115	23.9	82	21.75
0.6	1.126	24.9	82.5	23.17
0.8	1.119	24.3	81.8	22.24

Table S2 Summary of the modified SnO_2 based perovskite solar cells

ETL Type	μ_e (SnO_2)	μ_e (modified SnO_2)	Perovskite type	Year	PCE	Refs.
EDTA- SnO_2	9.92×10^{-4}	2.27×10^{-3}	FACsI	2018.8	21.6	[S1]
Nb-SnO_2	1.02×10^{-4}	2.16×10^{-4}	FAMAPbIBr	2016.12	17.57	[S2]
SnO_2–HP	1.52×10^{-3}	2.76×10^{-3}	CsFAMAPbIBr	2020.7	23.06	[S3]
SnOx: $NdCl_3$	1.46×10^{-3}	6.29×10^{-3}	$FA_{1-x}MA_xPbI_3$	2020.9	21.49	[S4]
SnO_2:GQDs	6.72×10^{-4}	1.01×10^{-3}	$MAPbI_3$	2017.8	20.31	[S5]
SnO_2-RCQs	9.32×10^{-4}	1.73×10^{-2}	CsFAMAPbIBr	2019.11	22.77	[S6]
G- SnO_2	5.2×10^{-3}	7.5×10^{-3}	CsFAMAPbIBr	2019.12	22.13	[S7]
S-SnO_2	3.37×10^{-4}	3.46×10^{-3}	FAMAPbIBr	2020.9	22.84	
Nd- SnO_2	12.1×10^{-4}	36.1×10^{-4}	CsFAMAPbIBr	2020.6	20.92	[S8]
cPCN-SnO_2	**9.95×10^{-4}**	**3.3×10^{-3}**	**FAMAPbIBr**	**2020.12**	**23.17**	**This work**

Supplementary References

[S1] D. Yang, R. Yang, K. Wang, C. Wu, X. Zhu et al., High efficiency planar-type perovskite solar cells with negligible hysteresis using EDTA-complexed SnO_2 Nat. Commun. **9**(1), 3239 (2018). https://doi.org/10.1038/s41467-018-05760-x

[S2] X. Ren, D. Yang, Z. Yang, J. Feng, X. Zhu et al., Solution-processed Nb: SnO_2 electron transport layer for efficient planar perovskite solar cells. ACS Appl. Mater. Interfaces **9**(3), 2421-2429 (2017). https://doi.org/10.1021/acsami.6b13362

[S3] S. You, H. Zeng, Z. Ku, X. Wang, Z. Wang et al., Multifunctional polymer-regulated SnO_2 nanocrystals enhance interface contact for efficient and stable planar

perovskite solar cells. Adv. Mater. **32**(43), e2003990 (2020). https://doi.org/10.1002/adma.202003990

[S4] Q. Xiong, L. Yang, Q. Zhou, T. Wu, C. L. Mai et al., $NdCl_3$ dose as a universal approach for high-efficiency perovskite solar cells based on low-temperature-processed snox. ACS Appl. Mater. Interfaces **12**(41), 46306-46316 (2020). https://doi.org/10.1021/acsami.0c13296

[S5] J. Xie, K. Huang, X. Yu, Z. Yang, K. Xiao et al., Enhanced electronic properties of SnO_2 via electron transfer from graphene quantum dots for efficient perovskite solar cells. ACS Nano **11**(9), 9176-9182 (2017). https://doi.org/10.1021/acsnano.7b04070

[S6] W. Hui, Y. Yang, Q. Xu, H. Gu, S. Feng et al., Red-carbon-quantum-dot-doped SnO_2 composite with enhanced electron mobility for efficient and stable perovskite solar cells. Adv. Mater. **32**(4), e1906374 (2020). https://doi.org/10.1002/adma.201906374

[S6] J. Chen, H. Dong, L. Zhang, J. Li, F. Jia et al., Graphitic carbon nitride doped SnO_2 enabling efficient perovskite solar cells with pces exceeding 22%. J. Mater. Chem. A **8**(5), 2644-2653 (2020). https://doi.org/10.1039/c9ta11344d

[S7] J. Jia, J. Dong, J. Wu, H. Wei, B. Cao, Combustion procedure deposited SnO_2 electron transport layers for high efficient perovskite solar cells. J. Alloys Compd. **844** 156032 (2020). https://doi.org/10.1016/j.jallcom.2020.156032